Biochemical Pharmacology 175 (2020) 113921

Contents lists available at ScienceDirect

Biochemical Pharmacology

journal homepage: www.elsevier.com/locate/biochempharm

Activation of notch 3/c-MYC/CHOP axis regulates apoptosis and promotes sensitivity of lung cancer cells to mTOR inhibitor everolimus

Ting Li[a], Xiao-Huang Xu[a], Xia Guo[a], Tao Yuan[b], Zheng-Hai Tang[a], Xiao-Ming Jiang[a], Yu-Lian Xu[a], Le-Le Zhang[a], Xiuping Chen[a], Hong Zhu[b], Jia-Jie Shi[a], Jin-Jian Lu[a,*]

[a] State Key Laboratory of Quality Research in Chinese Medicine, Institute of Chinese Medical Sciences, University of Macau, Macao, China
[b] Zhejiang Province Key Laboratory of Anti-Cancer Drug Research, College of Pharmaceutical Sciences, Zhejiang University, Hangzhou 310058, China

ARTICLE INFO

Keywords:
Lung cancer
Notch 3
c-MYC
CHOP
Apoptosis

ABSTRACT

The mammalian target of rapamycin (mTOR) pathway converges diverse environmental cues to support the lung cancer growth and survival. However, the mTOR-targeted mono-therapy does not achieve expected therapeutic effect. Here, we revealed that fangchinoline (FCL), an active alkaloid that purified from the traditional Chinese medicine *Stephania tetrandra* S. Moore, enhanced the anti-lung cancer effect of mTOR inhibitor everolimus (EVE). The combination of EVE and FCL was effective to activate Notch 3, and subsequently evoked its downstream target c-MYC. The blockage of Notch 3 signal by the molecular inhibitor of γ-secretase or siRNA of Notch 3 reduced the c-MYC expression and attenuated the combinational efficacy of EVE and FCL on cell apoptosis and proliferation. Moreover, the c-MYC could bind to the C/EBP homologous protein (CHOP) promoter and facilitate CHOP transcription. The conditional genetic deletion of CHOP reduced the apoptosis on lung cancer cells to the same degree as blockage of Notch 3/c-MYC axis, providing further evidence for that the Notch 3/c-MYC axis regulates the transcription of CHOP and finally induces apoptosis upon co-treatment of FCL and EVE in lung cancer cells. Overall, our findings, to the best of our knowledge, firstly link CHOP to Notch 3/c-MYC axis-dependent apoptosis and provide the Notch 3/c-MYC/CHOP activation as a promising strategy for mTOR-targeted combination therapy in lung cancer treatment.

1. Introduction

The mammalian target of rapamycin (mTOR) pathway converges the effects of growth factors and availability of nutrients and energy for the regulation of cellular growth and proliferation metabolism [1,2]. It is well established that mTOR signaling pathway is a central oncogenic pathway during the development of lung cancer [3–5]. Indeed, the mTOR signal is frequently dysregulated and overactive to stimulate cell proliferation [6]. Many mTOR inhibitors, including the allosteric mTOR inhibitors (e.g., rapamycin) and catalytic mTOR inhibitor (e.g., AZD8055), have been actively developed [7–10]. As the derivative of rapamycin and one of the most famous mTOR inhibitors, everolimus (EVE), has been therapeutic option for the patients with the advanced kidney cancer, breast cancer and lung original neuroendocrine tumors, and investigated in many clinical trials for patients with lung cancer. Although mTOR inhibitors are expected to provide great benefits for patients in the clinical treatment, unfortunately, they are showing slight therapeutic effect when used as mono-therapy. Consequently, the further knowledge of the molecular mechanisms governing cancer progression is essential to dissect and develop novel combinative approach for mTOR-targeted therapy.

The natural products and their derivatives have been a continuing source for drug discovery [11–16]. Fangchioline (FCL) is an active alkaloid that purified from the dried root of the traditional Chinese medicine *Stephania tetrandra* S. Moore. It possesses a wide range of biological properties, such as anti-diabetic [17], anti-inflammatory [18,19], as well as anti-cancer activities [20]. In our previous work, FCL was identified as a regulator of autophagy in lung cancer cells, however, whether FCL is an inducer or inhibitor depends on the treatment period. FCL mediated the autophagosome generation and stimulated autophagy in the early stage by promoting the TEFB nuclear translocation, while it restrained the autophagosomes degradation and inhibited autophagy in the late stage by blocking the autophagosomes–lysosomes fusion and lysosome function [21].

We here first discovered that the natural product FCL amplified the anti-lung cancer effect of the mTOR inhibitor EVE and that an activated

* Corresponding author at: State Key Laboratory of Quality Research in Chinese Medicine, Institute of Chinese Medical Sciences, University of Macau, 5005a, N22, Avenida da Universidade, Taipa, Macao, China.
E-mail addresses: jinjianlu@um.edu.mo, jinjian.lu@163.com (J.-J. Lu).

https://doi.org/10.1016/j.bcp.2020.113921
Received 31 December 2019; Accepted 17 March 2020
Available online 19 March 2020
0006-2952/

Notch 3-mediated apoptosis is essential for the combinative efficiency. Specifically, we also observed a strong link between c-MYC and CHOP for the modulation of apoptosis. Eventually, we demonstrated a novel Notch 3/c-MYC/CHOP pathway participating apoptosis induction in lung cancer cells, thus providing novel therapeutic approach for the mTOR-targeted combination therapy.

2. Materials and methods

2.1. Reagents

EVE (> 98%, PubChem CID: 57369482) was purchased from Selleck Chemicals (Houston, TX, USA), and FCL (> 98%, PubChem CID: 73481) were bought from the National Institutes for Food and Drug Control (Beijing, China). Compounds were dissolved in dimethylsulfoxide (DMSO) at a concentration of 40 mM, and stored at –20 °C as stock solutions. The compounds were then diluted in a culture medium containing final DMSO with concentrations not exceeding 0.1% before each experiment. Bovine serum albumin (BSA), MTT, chloroquine (CQ), 3-Methyladenine (3-MA), DMSO, phenylmethanesulfonyl fluoride (PMSF) were obtained from Sigma (Saint Louis, MO, USA). Roswell Park Memorial Institute (RPMI) 1640 medium, penicillin, streptomycin, fetal bovine serum (FBS), and phosphate-buffered saline (PBS) were obtained from Gibco Life Technologies (Grand Island, NY, USA). The protease and phosphatase inhibitor cocktail was bought from Thermo Fisher Scientific Inc. (Waltham, MA, USA). RIPA buffer, cleaved (ADP-ribose) polymerase (PARP), and c-caspase 3 antibodies were purchased from Beyotime Biotechnology (Shanghai, China). Z-VAD-FMK (zVAD), and Avagacestat (AVA) was purchased from Selleck Chemicals (Houston, TX, USA). Primary antibodies against Notch 1, Notch 3, c-MYC, CHOP, HES-1, p-4E-BP1 (S65), 4E-BP1, GAPDH, and anti-rabbit IgG HRP-conjugated secondary antibody were all purchased from Cell Signaling Technology (Beverly, MA, USA). Primers were prepared by Invitrogen Life Technologies (Shanghai, China) and the small interfering RNA (siRNA) were synthesized by GenePharma (Shanghai, China).

2.2. Cell lines and culture

Human lung cancer cells (A549, NCI-H1299, NCI-H358, HCC827, and NCI-H1975), and the human embryonic kidney cells (HEK293T) were obtained from American Type Culture Collection (ATCC, Rockville, MD, USA). The NCI-H1975/OSIR cells were the same as our previous study [22]. All lung cancer cell lines were grown in RPMI 1640 medium, and the HEK293T were maintained in the DMEM medium, both mediums were supplemented with 10% (v/v) FBS and antibiotics (100 units/mL penicillin and 100 μg/mL streptomycin). All cells were cultured in an incubator at 37 °C, 5% CO_2 and the 95% relative humidity according to the guidelines provided by the vendors.

For c-MYC-overexpressed NCI-H1975 cells, the related primers were designated with the restriction sites of EcoR I and Not I. The human c-MYC coding sequence (CDS) was amplified accordingly, and cloned into the EcoR I/Not I sites of the pCDH-puro plasmid. HEK293T cells were transfected with the pCDH-c-MYC-puro or empty vector. After 60 h incubation, the lentiviral particles were collected from supernatant and used to infect NCI-H1975 cells. Infected cells were then selected for > 7 days by incubation with puromycin and the c-MYC expression was verified by quantitative reverse transcriptase-PCR (qRT-PCR) and western blot assays. The stable c-MYC-overexpressed cells were maintained in medium containing 5 μg/ml puromycin.

2.3. MTT assay

Cells were plated into 96-well plates at a density of 6,000 cells per well. After 24 h adhesion, cells were treated with different concentrations of compounds diluted in a medium containing 0.5% FBS for another 12 h or 24 h. After that, 1 mg/mL MTT was added into the wells and incubated for 4 h. The medium was then discarded, and DMSO was added to dissolve the violet formazan crystals. The absorbance of the solution at 570 nm was recorded with a microplate reader (Perkin Elmer, 1420 Multilabel Counter Victor3, Wellesley, MA, USA).

2.4. Colony formation assay

Cells were planted into 6-well plates at a density of 500 cells per well. After 24 h of adhesion, cells were treated with compounds diluted in a medium containing 0.5% FBS for another 12 h. The supernatant was removed and the cells were then cultured in a medium containing 10% FBS for 1 week with renewal every 2 days. The cells were then stained by crystal violet and observed with an Axiovert 200 inverted microscope (Carl Zeiss, Jena, German).

2.5. Western blot analysis

Cells were planted into the 6-well plates for 24 h, and adhesive cells were treated with compounds diluted in a medium containing 0.5% FBS for another 24 h. The proteins were initially lysed with a RIPA buffer containing inhibitors. The specific protein bands were visualized with an ECL advanced Western blot assay detection kit (GE Healthcare, Uppsala, Sweden) as previously described [15].

2.6. Annexin V/PI staining

Cells were seeded into a 6-well plates and maintained in an incubator for 24 h and then treated with different concentrations of compounds diluted in the medium containing 0.5% FBS for 12 h or 24 h before harvested. Annexin V-FITC/PI apoptosis detection kit (BioVision, CA, USA). was used to detect the apoptotic cells in accordance with the manufacturer's instruction.

2.7. RNA isolation and qRT-PCR assays

TRIzol reagent (Invitrogen, NY, USA) was used to extract total RNA from the cells and SuperScriptTM III first strand cDNA synthesis kit (Toyobo, Osaka, Japan) was used to reverse-transcribe the extracted total RNA into single stranded cDNA. qRT-PCR was performed using SYBR Green PCR Master Mix (Applied Biosystems, NY, USA) on a Stratagene Mx3005P multiplex quantitative PCR system (Agilent Technologies, CA, USA). GAPDH was used as an internal control, and $2^{-\Delta\Delta CT}$ values were normalized to control levels. Each sample was analyzed in triplicate. The primer sequences used were presented in Table 1.

2.8. Transfection assay

Cells were seeded overnight in a 6-well plates the day before transfection and then cells were transfected with the specific siRNAs using Lipofectamine™ 2000 transfection reagent (Invitrogen Corp., Carlsbad, CA, USA) according to the manufacture's protocol. After that, cells were treated with defined compounds and the relative protein or mRNA levels were further measured. The sequences of targeted siRNAs were presented in Table 1.

2.9. Chromatin immunoprecipitation

Chromatin immunoprecipitation (ChIP) was performed on 10^6 NCI-H1975 cells that treated with or with 20 μM EVE and 10 μM FCL for 3 h. ChIP experiments were performed using Pierce™ Chromatin Prep Module Kit (Thermo Fisher Scientific Inc., RD, USA) according to the procedures provided by the manufacturer starting using normal rabbit IgG (Cell signal technology, #3900) or anti-c-MYC (Cell signal technology, #9402). The purified DNA precipitates were then used as

Table 1
Primer sequences.

Primer	Sequence
RT-qPCR primers	
NOTCH3 forward	TGACCGTACTGGCGAGACT
NOTCH3 reverse	CCGCTTGGCTGCATCAG
JAG1 forward	AGCGACCTGTGTGGATGAG
JAG1 reverse	GGCTGGAGACTGGAAGACC
JAG2 forward	TCTCTGTGAGGTGGATGTCG
JAG2 reverse	CAGTCGTCAATGTTCTCATGG
DLL1 forward	ACTCCTACCGCTTCGTGTGT
DLL1 reverse	ATGCTGCTCATCACATCCAG
DLL3 forward	TGAGCATGGCTTCTGTGAAC
DLL3 reverse	CATTCAAAGGACCTGGGTGT
DLL4 forward	GCACTCCCTGGCAATGTACT
DLL4 reverse	CTCCAGCTCACAGTCCACAC
c-myc forward	AAACACAAACTTGAACAGCTAC
c-myc reverse	ATTTGAGGCAGTTTACATTATGG
Hes1 forward	GAAGCACCTCCGGAACCT
Hes1 reverse	GTCACCTCGTTCATGCACTC
CHOP forward	TGGTATGAGGACCTGCAAGAG
CHOP reverse	AGTCAGCCAAGCCAGAGAAG
GAPDH forward	GCGACACCCACTCCTCCACCTTT
GAPDH reverse	TGCTGTAGCCAAATTCGTTGTCATA
siRNA primers	
Notch 3 sense	GCAGCGAUGGAAUGGGUUUTT
Notch 3 antisense	AAACCCAUUCCAUCGCUGCTT
c-MYC sense	GGACUAUCCUGCUGCCAAG
c-MYC antisense	CCUGAUAGGACGACGGUUC
CHOP sense	GUUUCCUGGUUCUCCCUUGGUCUUTT
CHOP antisense	AAGACCAAGGGAGAACCAGGAAACTT
ChIP-qPCR primers	
CHOP Primer Set 1 forward	CGACTAGGGGCGACCAAGGC
CHOP Primer Set 1 reverse	CTTCACGGAGGAGGTGGGTG
CHOP Primer Set 2 forward	AGACCTGTCATTGCCACACC
CHOP Primer Set 2 reverse	TGTGAAGGTAAAATGAGAAC
CHOP Primer Set 3 forward	CCCTGCCCCGCCCCAAAGGC
CHOP Primer Set 3 reverse	CAAGGCCGGTTGTGACTGGA

templates in qPCR reactions. The qPCR primer sequences were designed and used to amplify the DNA regions of human *CHOP* promoter: Set 1 (-214 to −452 containing the putative site at −327 to −338), Set 2 (-1444 to −1659 containing the putative site at −1545 to −1556), and Set 3 (-1618 to −1886 containing the putative site at −1759 to 1769). The sequences of the ChIP-qPCR primers were present in Table 1.

2.10. Statistical analysis

All experiments were repeated at least three times. Data were expressed as means ± SD. Statistical analysis was performed using Graph Pad Prism 8 (GraphPad Software, Inc., CA, USA). The protein bands and the colony forming cells were quantified using ImageJ software (1.49v, MD, USA). The *P* value stands for “statistically significant,” and the “ns” stands for “not statistically significant.” The *P* value stands for “statistically significant”, for instance, $*P < 0.05$: significant difference from control by analysis of variance, $**P < 0.01$: very significant difference from control by analysis of variance, $***P < 0.001$: highly significant difference from control by analysis of variance. “ns” stands for “not statistically significant”.

3. Results

3.1. The natural compound FCL enhances the anti-cancer effect of mTOR inhibitor EVE

The natural product FCL has been shown previously to be an autophagy regulator [21]. Given that the mTOR is the key factor of autophagy initiation, autophagy is reported to be triggered by the inhibition of mTOR activity and acts as a cell survival-promoting mechanism for tumors upon mTOR-targeted therapy [23,24]. We postulated that the autophagy regulator FCL could influence the anti-cancer potential of mTOR inhibitor. Several lung cancer cells lines, including NCI-H1975, HCC827, NCI-H358, NCI-H1299, A549, and the osimertinib (OSIR)-resistant NCI-H1975/OSIR cells, were firstly exposed to EVE and FCL and the cell proliferation was detected after indicated time points. As shown in Fig. 1A, co-treatment of mTOR inhibitor EVE and FCL obviously suppressed cell proliferation against these lung cancer cells, upon 24 h co-treatment. Elevated inhibitory effect on cell colony formation was also observed in the NCI-H1975 cells with this co-treatment (Fig. 1B). We next tested the sensitivity of NCI-H1975 cells to FCL and other mTOR inhibitors, such as temsirolimus and Torin 1, and found that the co-incubation of mTOR inhibitors and FCL also showed enhanced anti-cancer property in NCI-H1975 cells when compared with the mono-incubation of EVE or FCL during 24 h period (data not shown).

In line with a previous report, we uncovered that the autophagy marker LC3-II was increased after a single treatment with EVE or FCL and even more when combined, which indicates that single or combined treatment of FCL or EVE can regulate autophagy (Fig. 1C). To investigate if autophagy is causal to this combination, we tested whether pharmacological suppression of autophagy could reverse sensitivity to the combination of EVE and FCL in NCI-H1975 cells. However, the addition of autophagy inhibitors, CQ and 3-MA, did not reverse the combination-mediated growth inhibition, indicating the increasing sensitivity of cancer cells to the mTOR-targeted therapy is autophagy-independent (Fig. 1D).

Apoptosis is important type of programmed cell death [25,26]. We further evaluated whether apoptosis participated in the combinative effect of EVE and FCL. The cleaved caspase 3 and its downstream target PARP were classic apoptotic biomarkers [27,28], the apoptotic effect of FCL and EVE co-treatment was clearly detected with enhanced c-caspase 3 and c-PARP. In contrast, neither EVE nor FCL mono-treated lung cancer cells were detected with increased caspase 3 and PARP cleavage (Fig. 1E). In addition, by using Annexin V-FITC/PI staining assay, we observed that FCL or EVE alone had little effect on apoptosis, while the combination of EVE and FCL induced a visible apoptosis in a time-dependent manner (Fig. 1F). Validating this, the addition of the pan-caspases inhibitor zVAD attenuated the apoptotic promotion and proliferative inhibition mediated by the combination of EVE and FCL (Fig. 1G, 1H and 1I). Taken together, the ability of FCL to potentiate EVE-caused cell proliferative suppression depends on the regulation of cell apoptosis.

3.2. Notch 3 correlates with EVE and FCL-mediated anti-lung cancer effect

Besides autophagy, another well-known mechanism underlying the resistance of mTOR targeted therapy is the feedback increased expression of some membrane receptors [29–35]. First of all, the mTOR target, 4E-BP1, was significantly inhibited by EVE treatment and slightly inhibited by FCL treatment, but was not further affected by the combination of EVE and FCL, which indicates that in this study, the inhibitory activity on mTOR may not be so important for FCL function, nor is it the main reason for the enhanced efficacy of this combination (Fig. 2A). Epidermal growth factor receptor (EGFR), a common mutant and driven gene in lung cancer [36,37], is one of the classic mTOR feedback factors [14,38], but no further increase in expression was found in the combination group (data not shown). Other membrane-bound receptors have also been reported to be associated with mTOR resistance. For example, Notch 1 has been described as contributing to the resistance of mTOR inhibitors [39], and certain family members, especially Notch 3, appear to be key molecules that are frequently overexpressed in lung cancer cells [40,41]. We thus investigated whether Notch signal influences the combinative capability in lung cancer cells. As shown in Fig. 2B, Notch 1 and Notch 3 were slightly inducible upon either mono-treatment of EVE or FCL, however, it was Notch 3 that further increased upon the co-treatment of EVE and FCL.

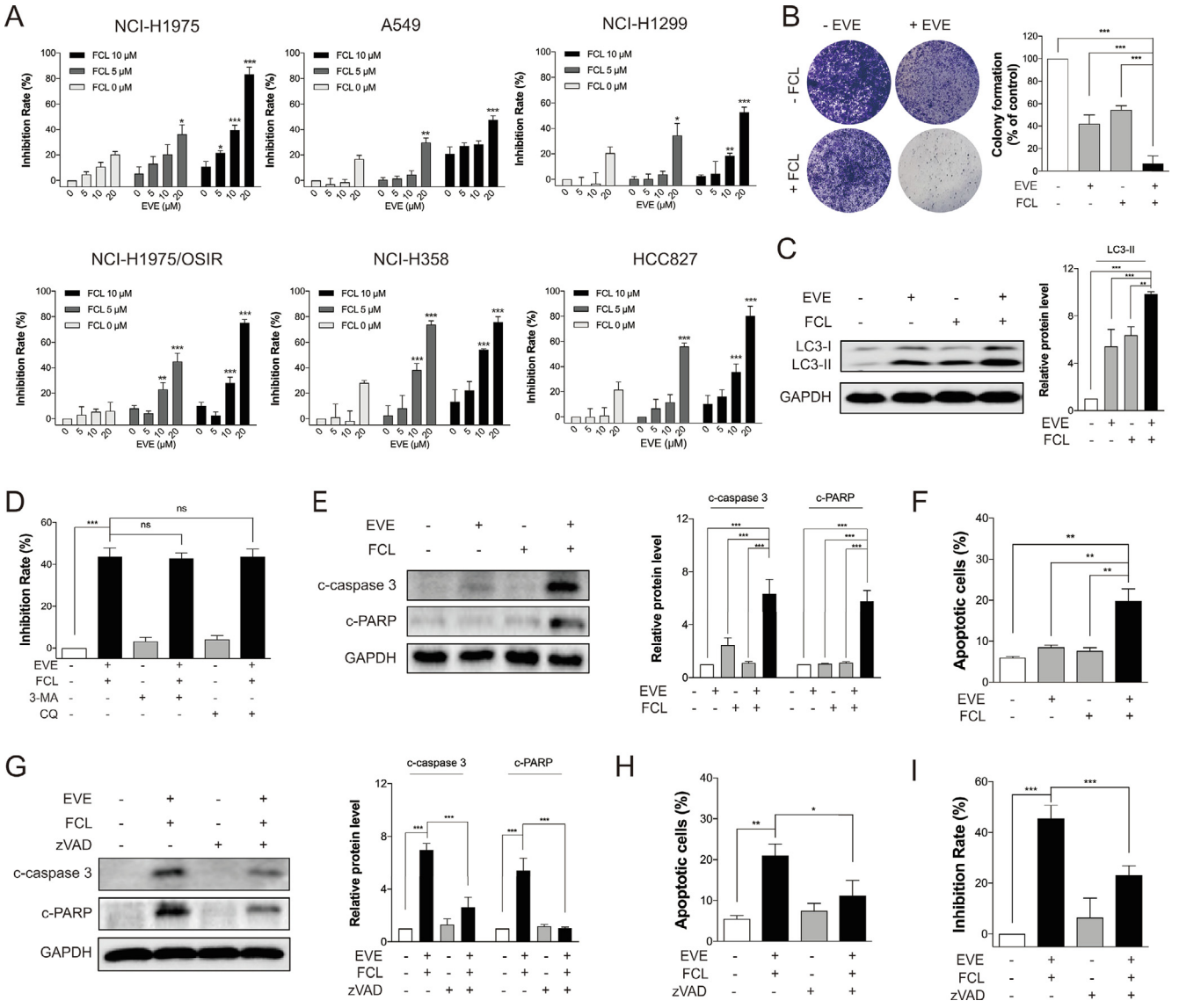

Fig. 1. FCL enhances the anti-cancer effect of mTOR inhibitor EVE. Lung cancer cells were treated with the indicated concentrations of EVE with or without FCL for 24 h. The cell viability was evaluated by MTT assay (A). NCI-H1975 cells were treated with the indicated concentrations of EVE and FCL, the cell colony formation activity was evaluated (B), and the levels of relative proteins were analyzed using Western blotting assay (C and E). NCI-H1975 cells were pre-treated with autophagy inhibitors, 3-MA and CQ, for 1 h, and co-treated with EVE and FCL for another 12 h, and the cell proliferation was evaluated using MTT assays (D). NCI-H1975 cells were treated with EVE and/or FCL, and the apoptotic cells were then analyzed (F). NCI-H1975 cells were pre-treated with pan-caspases inhibitor Z-VAD-FMK (10 μM) for 1 h, and co-treated with EVE and FCL for another 12 h. The levels of relative proteins were analyzed using Western blotting assay (G), apoptotic cells were stained with Annexin V/PI and analyzed by flow cytometry (H), and the cell proliferation was evaluated using MTT assays (I). $*P < 0.05$, $**P < 0.01$, and $***P < 0.001$. The "ns" stands for "not statistically significant". The lane without EVE and FCL is vehicle group.

To confirm whether the upregulation of Notch 3 was related to the increased transcriptional activity, we detected the mRNA levels of Notch 3 and found that neither mono-treatment nor co-treatment with EVE and FCL could affect the transcriptional level of Notch 3 by using the qRT-PCR assay (Fig. 2B). Of interest, the Notch 3 activity at known gene transcription, such as *Hes1* and *c-myc* [42–44], was modulated by the combination of EVE and FCL (Fig. 2C). The significantly increased HES-1 and c-MYC protein levels were also confirmed with the EVE and FCL co-incubation (Fig. 2B), validating the specific effects of EVE and FCL combination on the Notch 3 activity.

Using specific siRNAs to mediate the depletion of Notch 3, we set out to determine the need for Notch 3 in the combined activity of EVE and FCL. As expected, knockdown of Notch 3 led to marked reduction of apoptotic effect with EVE and FCL co-treatment, as evidenced by the decreased levels of apoptotic markers, i.e. c-caspase 3 and c-PARP, and reduced percentage of apoptotic cells (Fig. 2D and 2E). The attenuated apoptotic effect resulted in decreased proliferative suppression (Fig. 2F). Therefore, the membrane receptor Notch 3 may play a key role in the regulation of apoptosis mediated by co-treatment of EVE and FCL.

3.3. The EVE and FCL-mediated anti-cancer effect is correlated with the γ-secretase activity

This Notch pathway is initiated between neighboring cells via the interaction of ligand-receptor [45]. We first wanted to uncover if the increased activity of Notch 3 was related to the increased level of Notch ligands. Of note, the exposure to the EVE and FCL, alone or together, did not severely impacted the levels of Notch ligands (Fig. 3A).

We next assessed whether the pharmacological inhibition of γ-secretase, which mediates the Notch 3 cleavage and activation, could abolish the anti-cancer effect of the combination of EVE and FCL. We

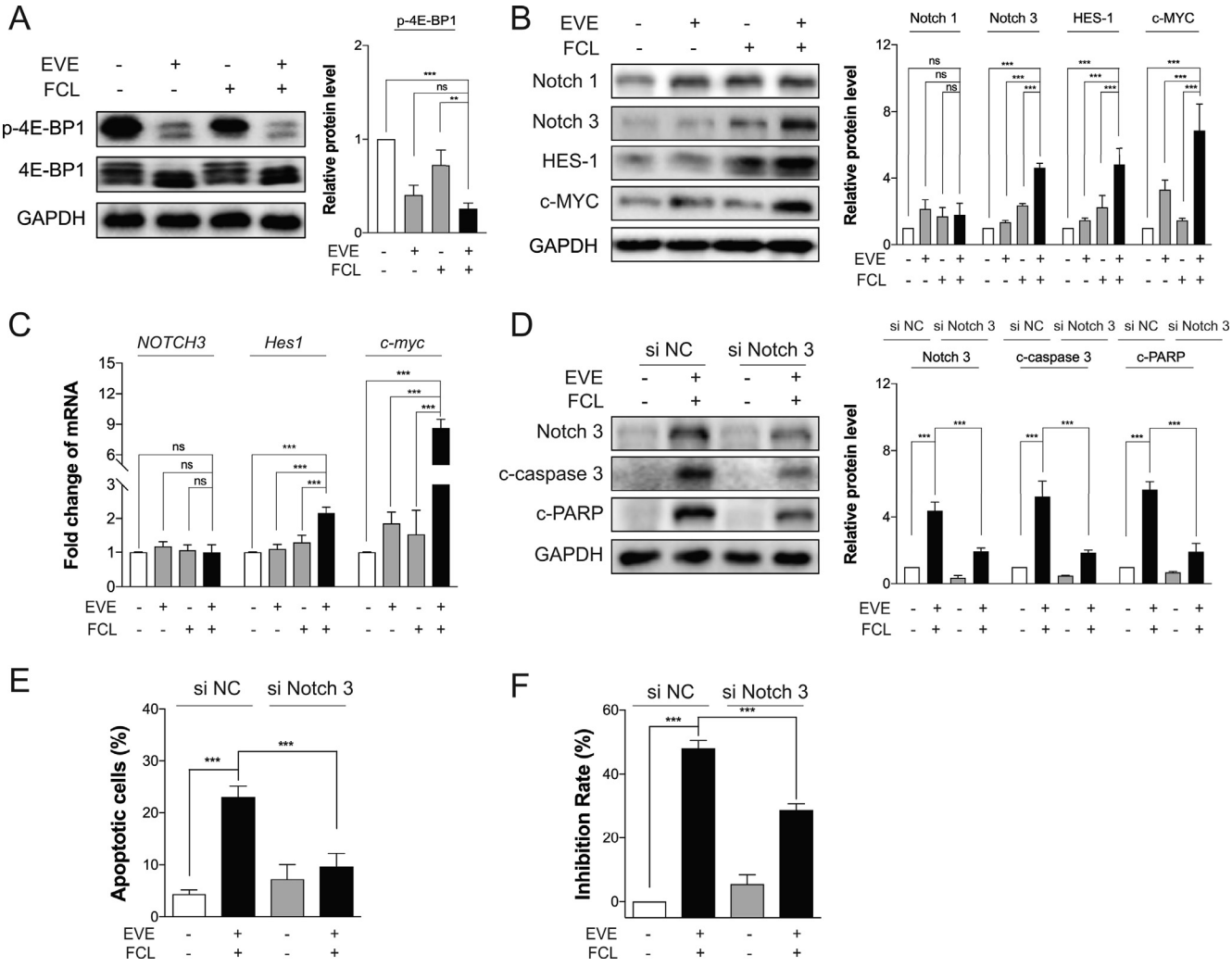

Fig. 2. Notch 3 correlates with EVE and FCL-mediated anti-lung cancer effect. The NCI-H1975 cells were treated the indicated concentrations of EVE and FCL. The levels of relative proteins were analyzed using Western blotting assay after 12 h treatment (A and B), the mRNA levels relative proteins were analyzed using qRT-PCR after 3 h treatment (C). Upon the knockdown of Notch 3 using specific siRNA, the NCI-H1975 cells were co-treated with EVE and FCL for 12 h. The levels of relative proteins were analyzed using Western blotting assay (D), The apoptotic cells were stained with Annexin V/PI and analyzed by flow cytometry (E), and the cell proliferation was evaluated using MTT assays (F).

pre-treated NCI-H1975 cells with the γ-secretase inhibitor AVA [46] for 1 h before the addition of EVE and FCL. As shown in Fig. 3B, the AVA pre-treatment could inhibit the activity of Notch 3 pathway with reduction of Notch 3, HES-1 and c-MYC. Inhibition of the Notch 3 by AVA resulted in the reversal of EVE and FCL combination-mediated apoptosis as determined by the decreased c-caspase 3 and c-PARP (Fig. 3C) and the reduced apoptotic cells (Fig. 3D). Subsequently, a statistically significant reduction in cell viability inhibition in EVE and FCL co-treated cells was observed (Fig. 3E). Consistent with the above data, the AVA pre-treatment could inhibit the activity of Notch 3 pathway, led the reversal of apoptosis in other lung cancer cell lines, including NCI-H1975/OSIR, HCC827 (data not shown). Overall, these results demonstrate that the Notch 3 was probably induced by the γ-secretase activation upon EVE and FCL treatment.

3.4. c-MYC is an essential operator of Notch 3-controlling anti-cancer effect

The c-MYC is a well-known target of Notch family [47], as well as a pioneer transcription factor playing critical roles in cell apoptosis [48], which promoted us to interrogate the role of c-MYC in the Notch 3-mediated apoptosis. Indeed, knocking down c-MYC by using targeted siRNA diminished the EVE and FCL co-treatment-induced cell apoptosis to a similar level as the Notch 3 blockade did in NCI-H1975 cells (Fig. 4A and 4B). The attenuated apoptotic effect by the c-MYC deletion eventually reduced the inhibition effect on cell viability by the co-treatment of EVE and FCL (Fig. 4C).

To test the positive correlation between c-MYC expression and anti-lung cancer activity of EVE and FCL, we established a c-MYC-over-expressed NCI-H1975 cell line and detected whether c-MYC expression influenced cell sensitivity to EVE and FCL. In keeping with our above findings, NCI-H1975 cells with higher c-MYC level were more susceptible to cell apoptosis in the co-treatment of EVE and FCL (Fig. 4D and E). In the end, the amplified apoptosis caused an enhanced anti-lung cancer effect of EVE plus FCL. The abovementioned results demonstrated that the Notch 3-induced combinative effect of the co-treatment of EVE and FCL relies on the downstream factor c-MYC.

3.5. CHOP is the downstream of Notch3-c-MYC axis

Having confirmed that the Notch 3/c-MYC signal correlates with the combinative activity of EVE and FCL, we next interrogated the downstream factor of Notch 3/c-MYC axis. By screening several c-MYC related factors, we happened to observe that c-MYC positively associated with the cellular level of CHOP, which is a core effector of programmed

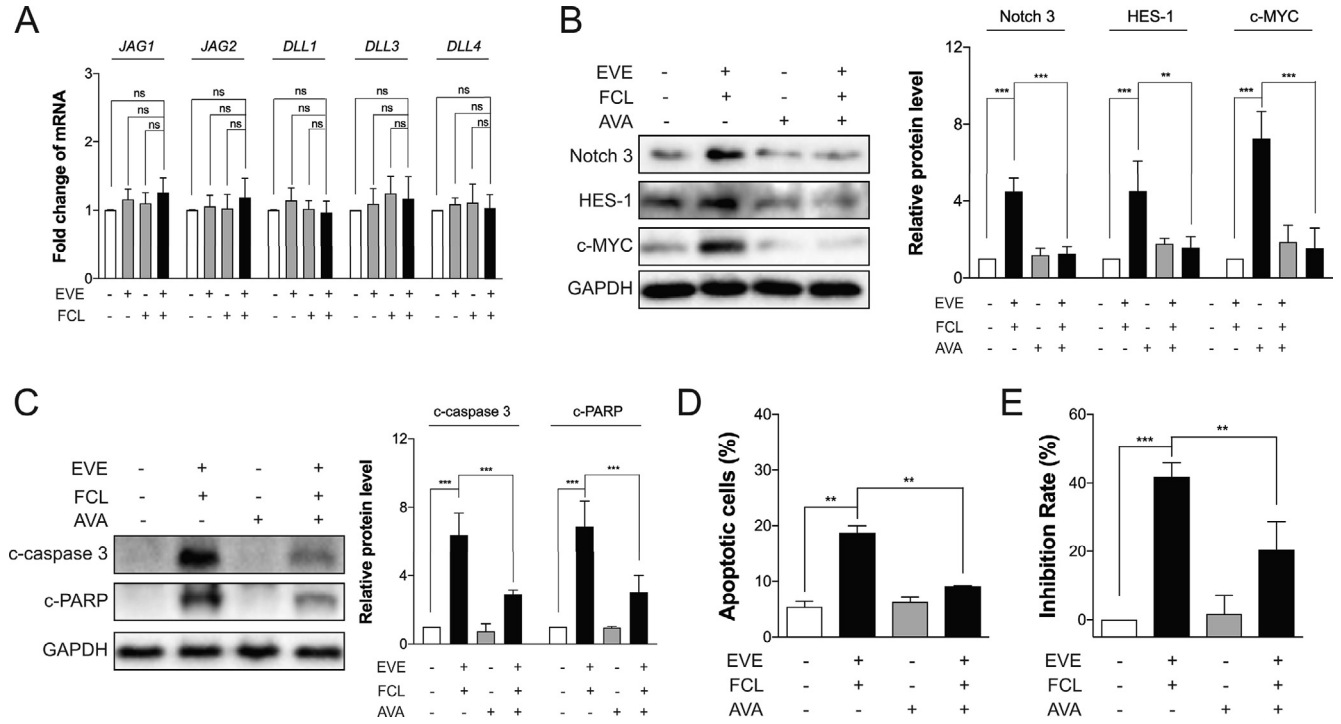

Fig. 3. The EVE and FCL-mediated anti-cancer effect is correlated with the γ-secretase activity. After treated with EVE and/or FCL for 3 h, the mRNA levels of relative proteins were analyzed by using qRT-PCR assay (A). After pre-treated with the γ-secretase inhibitor, AVA, for 1 h, the NCI-H1975 cells were co-treated with EVE and FCL for another 12 h. Then the levels of relative proteins were analyzed using Western blotting assay (B and C), the apoptotic cells were stained with Annexin V/PI and analyzed by flow cytometry (D), and the cell proliferation was evaluated using MTT assays (E).

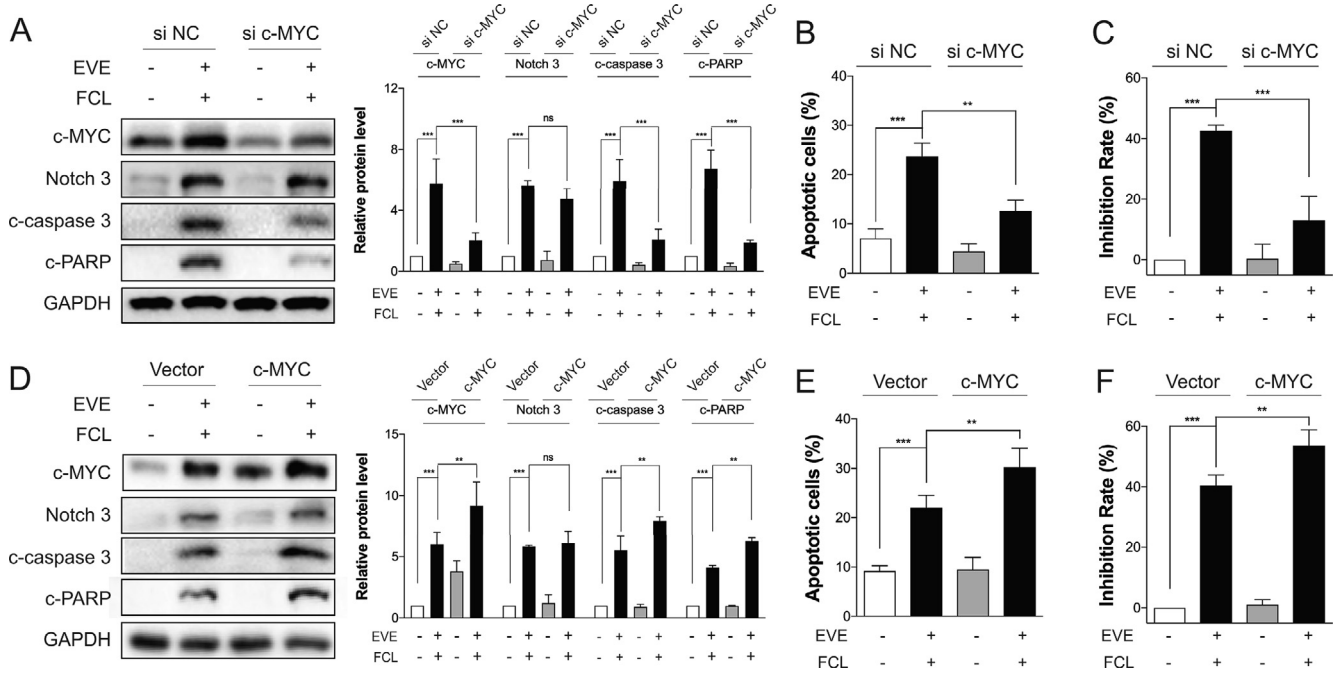

Fig. 4. c-MYC is an essential operator of Notch 3-controlling anti-cancer effect. After knockdown of c-MYC, the NCI-H1975 cells were treated with EVE and/or FCL for 12 h. The levels of relative proteins were analyzed using Western blotting assay (A), the apoptotic cells were stained with Annexin V/PI and analyzed by flow cytometry (B), and the cell proliferation was evaluated using MTT assays (C). The c-MYC-overexpressed NCI-H1975 cells were treated with EVE and/or FCL for 12 h. The levels of relative proteins were analyzed using Western blotting assay (D), the apoptotic cells were stained with Annexin V/PI and analyzed by flow cytometry (E), and the cell proliferation was evaluated using MTT assays (F).

cell death. Knockdown of c-MYC decreased both the mRNA level and protein level of CHOP, while knockdown of CHOP did not significantly influence the levels of Notch 3 and c-MYC (Fig. 5A and B).

Our finding that c-MYC-controlled the level of CHOP promoted us to determine if c-MYC plays a direct role in the transcription of CHOP. Firstly, three c-MYC binding motifs within the CHOP promoter were predicted, suggesting that the c-MYC shows potential that binds to the CHOP promoter (Fig. 5C). The chromatin immunoprecipitation assay

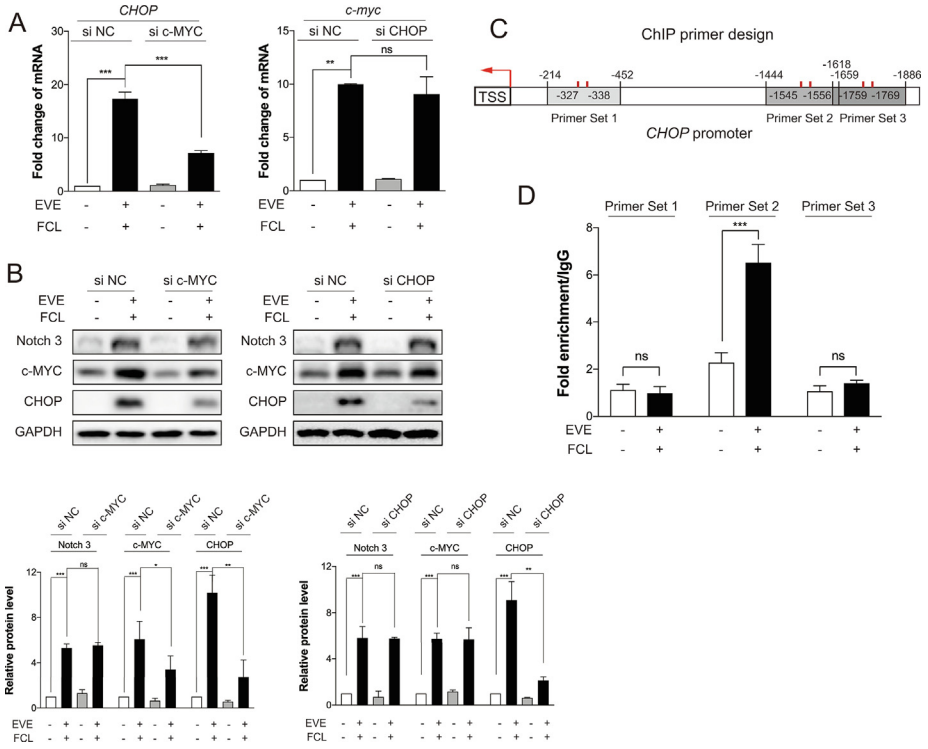

Fig. 5. CHOP is the downstream of Notch3-c-MYC axis. After knockdown of c-MYC or CHOP, the cells were treated with EVE and/or FCL, the mRNA levels of relative protein were analyzed by using qRT-PCR assay after 3 h treatment (A), and the levels of relative proteins were analyzed by using Western blotting assay after 12 h treatment (B). Schematic of CHOP transcriptional start site (TSS) and 0 to 2000 bp upstream sequence. Design of qPCR products for chromatin immunoprecipitation (ChIP) experiments and predicted c-MYC binding sites (red) are indicated (C). ChIP-qPCR detection of c-MYC binding to the CHOP promoter region. Relative amplification of primer sets indicated in (C) precipitated by either anti- c-MYC or anti-IgG antibodies are plotted (D). (For interpretation of the references to colour in this figure legend, the reader is referred to the web version of this article.)

with an anti-c-MYC antibody was then performed. As showed in the Fig. 5D, endogenous c-MYC precipitated with the genomic CHOP promoter sequence surrounding at only one of the predicted binding sites.

Collectively, these observations suggest that c-MYC binds the CHOP promoter during the co-treatment of EVE and FCL and may play a role in its induced transcriptional expression, and that CHOP was further confirmed as a positive target of c-MYC.

3.6. A functional Notch 3/c-MYC/CHOP axis is required for the combinative effect of EVE and FCL

Indeed, the co-treatment of EVE and FCL elevated the CHOP at both mRNA and protein levels remarkably (Fig. 6A and B). As expected, the elevated CHOP was found to be reduced by the Notch 3 inhibition (Fig. 6C). To ascertain the need of CHOP in the apoptosis induced by Notch 3/c-MYC signaling, we used the siRNA to knock down CHOP in NCI-H1975 cells. Consistent with the previous established role as downstream of Notch 3-c-MYC, we found that knockdown of CHOP suppressed the combinative activity of EVE and FCL, as determined by the reduced c-PARP and c-caspase 3 levels (Fig. 6D) and apoptotic cells (Fig. 6E), which eventually led to an attenuated anti-lung cancer effect (Fig. 6F). Together, these data establish that CHOP contributes to anti-proliferative and apoptotic effect mediated by the co-treatment of EVE and FCL.

4. Discussion

In this study, we revealed that Notch 3 activation in lung cancer cells results in exquisite susceptibility to the combination of mTOR inhibitors (e.g, EVE, temsirolimus and Torin 1) and the natural product FCL. Our study also highlighted a functional role of Notch 3/c-MYC/CHOP signal as an essential effector of cell apoptosis. We first showed that the combination of mTOR inhibitor and FCL is sufficient to inhibit growth of lung cancer cells. And the membrane receptor Notch 3 regulates c-MYC expression and activation of c-MYC-dependent apoptosis is essential for the Notch 3-mediated growth of lung cancer cells. In addition, this c-MYC regulatory activity is reflected by the transcription of CHOP, possibly highlighting a novel mechanism involved in cell apoptosis.

The mTOR inhibitor was reported to activate Notch 1 in breast cancer cells, which helped the cancer cells escape death and led to limited efficiency of mTOR inhibitor [39]. It is tempting to speculate that the potential benefits of combining both current Notch 1 and mTOR inhibitors would lead to a better treatment of cancer. Here, we surprisingly found that it was the Notch 3, but not the closely related Notch 1 or other Notch receptors, was significantly associated with lung cancer cell apoptosis. Even though the four mammalian Notch receptors, Notch1, Notch 2, Notch 3, and Notch 4 are thought to mediate the core Notch signal in evolutionarily and mechanistically conserved manner, the increasingly evidence has suggested that they exhibit distinct non-overlapping functions [49–54]. In fact, the co-treatment of EVE and FCL did not further affect the Notch1, Notch 2 and Notch 4 (data not shown), instead, facilitated Notch 3 when compared to the mono-treatment of EVE and FCL. In lung cancer, the outcome of Notch 3 activation has been reported to be closely linked to the cellular context, indicating both oncogenic and tumor suppressed abilities of Notch 3 [42,55–58]. In our study, blockade of Notch 3 by either siRNA or by the related inhibitor attenuated the apoptotic response and reversed cell proliferative inhibition in various lung cancer cell lines, indicating that Notch 3 plays a crucial role in regulating cell apoptosis, and contributes to tumor suppression in lung cancer.

c-MYC, a classic downstream of the Notch pathway [47], was indeed regulated by Notch 3 in this study, and its effects on apoptosis and cell growth were similar to Notch 3. Lung cancer cell lines with increasing c-MYC seemed to be more sensitive to the co-treatment of EVE and FCL, which was in line with the previous reports that c-MYC is related to the regulation of cell apoptosis [48,59,60]. However, other findings also showed that c-MYC is an oncogene in some tumor cells and respond to cellular stimuli to control cell survival and growth [60]. How elevated c-MYC levels can have two opposite effects on cell growth is thus interesting. Multiple evidences suggests that c-MYC acts as an amplifier of expression at universal genes, and regulates cell growth primarily through this global protein transcription [61,62]. Therefore, when different downstream targets are activated in response to cellular

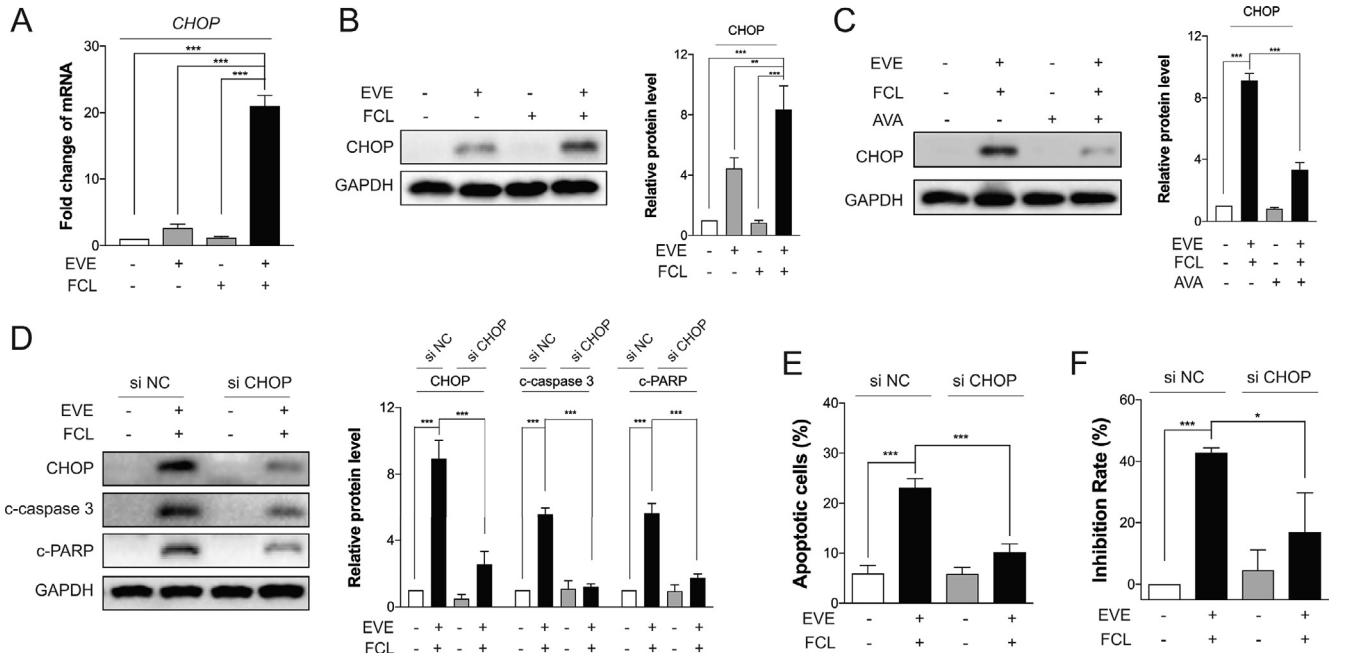

Fig. 6. A functional Notch 3/c-MYC/CHOP axis is required for the combinative effect of EVE and FCL. The NCI-H1975 cells were treated with EVE and/or FCL. The mRNA levels of relative proteins were analyzed using qRT-PCR after 3 h treatment (A), and the levels of relative proteins were analyzed using Western blotting assay after 12 h treatment (B). After pre-treated with the γ-secretase inhibitor, AVA, for 1 h, the NCI-H1975 cells were co-treated with EVE and FCL for another 12 h. Then the level of CHOP was analyzed using Western blotting assay (C). After knockdown of CHOP , the cells were co-treated with EVE and FCL for 12 h, the levels of relative proteins were analyzed by using Western blotting assay (D), the apoptotic cells were stained with Annexin V/PI and analyzed by flow cytometry (E), and the cell proliferation was evaluated using MTT assays (F).

stimuli, the role of c-MYC will be different. Previous studies have suggested that c-MYC functions upstream of CHOP and is inversely correlated with the CHOP transcription [63,64]. Strikingly, our results indicated that the c-MYC binds the CHOP promoter and positively regulate the CHOP transcription during the co-treatment of EVE and FCL. This novel finding in our study is that CHOP can also be a positive target of c-MYC. It was then shown that increased CHOP transcription contributes to subsequent apoptosis and is a major molecular component of Notch 3/c-MYC signaling. This study thus revealed an unexpected function of c-MYC and underscored a paradigm shift from Notch 3 to CHOP as being the master regulator of cell apoptosis during lung cancer treatment. Given the positive association between c-MYC and CHOP, detection of CHOP may be a potential indicator for c-MYC function and specifically targeting the Notch 3/c-MYC/CHOP could offer a novel therapeutic avenue for lung cancer management.

In summary, our findings uncovers a novel mechanism by which Notch 3 drives the apoptosis via modulating the downstream c-MYC and CHOP, therefore firstly linking CHOP to Notch 3/c-MYC axis and providing the Notch 3/c-MYC/CHOP activation as a promising strategy for mTOR-targeted combination therapy in lung cancer treatment.

CRediT authorship contribution statement

Ting Li: Conceptualization, Methodology, Investigation, Data curation, Writing - original draft, Writing - review & editing. **Xiao-Huang Xu:** Methodology, Investigation, Writing - review & editing. **Xia Guo**: Methodology, Investigation, Writing - review & editing. **Tao Yuan:** Methodology, Investigation, Writing - review & editing. **Zheng-Hai Tang:** Conceptualization, Methodology, Writing - review & editing. **Xiao-Ming Jiang**: Methodology, Writing - review & editing. **Yu-Lian Xu:** Methodology, Resources, Writing - review & editing. **Le-Le Zhang:** Methodology, Writing - review & editing. **Xiuping Chen:** Data curation, Writing - review & editing. **Hong Zhu:** Methodology, Writing - review & editing. **Jia-Jie Shi:** Writing - review & editing. **Jin-Jian Lu:** Methodology, Data curation, Supervision, Project administration, Funding acquisition, Writing - original draft, Writing - review & editing.

Declaration of Competing Interest

The authors declare that they have no known competing financial interests or personal relationships that could have appeared to influence the work reported in this paper.

Acknowledgements

We thank Prof. Ying Zheng and Ms. Run Han for the technical assistance. This work was supported by Science and Technology Development Fund, Macao S.A.R (FDCT) [024/2016/A1], the Research Fund of University of Macau [MYRG2018-00165-ICMS, MYRG2015-00091-ICMS-QRCM and MYRG2015-00101-ICMS-QRCM], National Natural Science Foundation of China [81973516].

Author contributions

T.L. and J.J.L conceived and designed the study. T.L., X.X.H, and X.G. performed the experiments. T.L., Z.H.T, and J.J.L analyzed and interpreted data. T.L. and J.J.L wrote the manuscript. All authors reviewed and approved the manuscript.

References

[1] J. Chung, C.J. Kuo, G.R. Crabtree, J. Blenis, Rapamycin Fkbp specifically blocks growth-dependent activation of and signaling by the 70 Kd S6 protein-kinases, Cell 69 (1992) 1227–1236.
[2] R.A. Saxton, D.M. Sabatini, mTOR signaling in growth, metabolism, and disease, Cell 168 (2017) 960–976.
[3] S. Ekman, M.W. Wynes, F.R. Hirsch, The mTOR pathway in lung cancer and implications for therapy and biomarker analysis, J Thorac. Oncol. 7 (2012) 947–953.
[4] E. Ilagan, B.D. Manning, Emerging role of mTOR in the response to cancer therapeutics, Trends Cancer. 2 (2016) 241–251.
[5] H. Cheng, M. Shcherba, G. Pendurti, Y. Liang, B. Piperdi, R. Perez-Soler, Targeting the PI3K/AKT/mTOR pathway: potential for lung cancer treatment, Lung Cancer Manag. 3 (2014) 67–75.

[6] N. Wagle, B.C. Grabiner, E.M. Van Allen, E. Hodis, S. Jacobus, J.G. Supko, et al., Activating mTOR mutations in a patient with an extraordinary response on a phase I trial of everolimus and pazopanib, Cancer Discov. 4 (2014) 546–553.

[7] I. Beuvink, A. Boulay, S. Fumagalli, F. Zilbermann, S. Ruetz, T. O'Reilly, et al., The mTOR inhibitor RAD001 sensitizes tumor cells to DNA-damaged induced apoptosis through inhibition of p21 translation, Cell 120 (2005) 747–759.

[8] D.S. Mortensen, K.E. Fultz, S. Xu, W. Xu, G. Packard, G. Khambatta, J.C. Gamez, J. Leisten, J. Zhao, J. Apuy, K. Ghoreishi, M. Hickman, R.K. Narla, R. Bissonette, S. Richardson, S.X. Peng, S. Perrin-Ninkovic, T. Tran, T. Shi, W.Q. Yang, Z. Tong, B.E. Cathers, M.F. Moghaddam, S.S. Canan, P. Worland, S. Sankar, H.K. Raymon, CC-223, a potent and selective inhibitor of mtor kinase: in vitro and in vivo characterization, Mol. Cancer Therap. 14 (6) (2015) 1295–1305.

[9] C.M. Chresta, B.R. Davies, I. Hickson, T. Harding, S. Cosulich, S.E. Critchlow, et al., AZD8055 is a potent, selective, and orally bioavailable ATP-competitive mammalian target of rapamycin kinase inhibitor with in vitro and in vivo antitumor activity, Cancer Res. 70 (2010) 288–298.

[10] S.M. Maira, F. Stauffer, J. Brueggen, P. Furet, C. Schnell, C. Fritsch, et al., Identification and characterization of NVP-BEZ235, a new orally available dual phosphatidylinositol 3-kinase/mammalian target of rapamycin inhibitor with potent in vivo antitumor activity, Mol. Cancer Ther. 7 (2008) 1851–1863.

[11] M.Y. Huang, L.L. Zhang, J. Ding, J.J. Lu, Anticancer drug discovery from Chinese medicinal herbs, Chin Med. 13 (2018) 35.

[12] Q. Li, Y. Niu, P. Xing, C. Wang, Bioactive polysaccharides from natural resources including Chinese medicinal herbs on tissue repair, Chin Med. 13 (2018) 7.

[13] L. Lu, W. Hu, Z. Tian, D. Yuan, G. Yi, Y. Zhou, et al., Developing natural products as potential anti-biofilm agents, Chin Med. 14 (2019) 11.

[14] T. Li, X. Chen, X.Y. Dai, B. Wei, Q.J. Weng, X. Chen, et al., Novel Hsp90 inhibitor platycodin D disrupts Hsp90/Cdc37 complex and enhances the anticancer effect of mTOR inhibitor, Toxicol Appl Pharmacol. 330 (2017) 65–73.

[15] T. Li, X. Chen, X. Chen, D.L. Ma, C.H. Leung, J.J. Lu, Platycodin D potentiates proliferation inhibition and apoptosis induction upon AKT inhibition via feedback blockade in non-small cell lung cancer cells, Sci Rep. 6 (2016) 37997.

[16] Z.H. Tang, T. Li, H.W. Gao, W. Sun, X.P. Chen, Y.T. Wang, et al., Platycodin D from platycodonis radix enhances the anti-proliferative effects of doxorubicin on breast cancer MCF-7 and MDA-MB-231 cells, Chin Med. 9 (2014) 16.

[17] T. Tsutsumi, S. Kobayashi, Y.Y. Liu, H. Kontani, Anti-hyperglycemic effect of fangchinoline isolated from Stephania tetrandra Radix in streptozotocin-diabetic mice, Biol Pharm Bull. 26 (2003) 313–317.

[18] Y.C. Shen, C.J. Chou, W.F. Chiou, C.F. Chen, Anti-inflammatory effects of the partially purified extract of radix Stephaniae tetrandrae: Comparative studies of its active principles tetrandrine and fangchinoline on human polymorphonuclear leukocyte functions, Mol. Pharmacol. 60 (2001) 1083–1090.

[19] H.S. Choi, H.S. Kim, K.R. Min, Y. Kim, H.K. Lim, Y.K. Chang, et al., Anti-inflammatory effects of fangchinoline and tetrandrine, J Ethnopharmacol. 69 (2000) 173–179.

[20] H.S. Lee, S. Safe, S.O. Lee, Inactivation of the orphan nuclear receptor NR4A1 contributes to apoptosis induction by fangchinoline in pancreatic cancer cells, Toxicol Appl Pharm. 332 (2017) 32–39.

[21] Z.H. Tang, X. Guo, W.X. Cao, X.P. Chen, J.J. Lu, Fangchinoline accumulates autophagosomes by inhibiting autophagic degradation and promoting TFEB nuclear translocation, Rsc Adv. 7 (2017) 42597–42605.

[22] Z.H. Tang, X.M. Jiang, X. Guo, C.M. Fong, X. Chen, J.J. Lu, Characterization of osimertinib (AZD9291)-resistant non-small cell lung cancer NCI-H1975/OSIR cell line, Oncotarget. 7 (2016) 81598–81610.

[23] B. Ravikumar, C. Vacher, Z. Berger, J.E. Davies, S.Q. Luo, L.G. Oroz, et al., Inhibition of mTOR induces autophagy and reduces toxicity of polyglutamine expansions in fly and mouse models of Huntington disease, Nat Genet. 36 (2004) 585–595.

[24] L. Yu, C.K. McPhee, L.X. Zheng, G.A. Mardones, Y.G. Rong, J.Y. Peng, et al., Termination of autophagy and reformation of lysosomes regulated by mTOR, Nature 465 (2010) 942–U11.

[25] G. Marino, M. Niso-Santano, E.H. Baehrecke, G. Kroemer, Self-consumption: the interplay of autophagy and apoptosis, Nat Rev Mol Cell Bio. 15 (2014) 81–94.

[26] L. Galluzzi, S.A. Aaronson, J. Abrams, E.S. Alnemri, D.W. Andrews, E.H. Baehrecke, et al., Guidelines for the use and interpretation of assays for monitoring cell death in higher eukaryotes, Cell Death Differ. 16 (2009) 1093–1107.

[27] A.H. Boulares, A.G. Yakovlev, V. Ivanova, B.A. Stoica, G.P. Wang, S. Iyer, et al., Role of poly(ADP-ribose) polymerase (PARP) cleavage in apoptosis - Caspase 3-resistant PARP mutant increases rates of apoptosis in transfected cells, J. Biol. Chem. 274 (1999) 22932–22940.

[28] A.G. Porter, R.U. Janicke, Emerging roles of caspase-3 in apoptosis, Cell Death Differ. 6 (1999) 99–104.

[29] K.E. O'Reilly, F. Rojo, Q.B. She, D. Solit, G.B. Mills, D. Smith, et al., mTOR inhibition induces upstream receptor tyrosine kinase signaling and activates Akt, Cancer Res. 66 (2006) 1500–1508.

[30] V.S. Rodrik-Outmezguine, S. Chandarlapaty, N.C. Pagano, P.I. Poulikakos, M. Scaltriti, E. Moskatel, et al., mTOR kinase inhibition causes feedback-dependent biphasic regulation of AKT signaling, Cancer Discov. 1 (2011) 248–259.

[31] H.B. Zhang, N. Bajraszewski, E.X. Wu, H.W. Wang, A.P. Moseman, S.L. Dabora, et al., PDGFRs are critical for PI3K/Akt activation and negatively regulated by mTOR, J. Clin. Invest. 117 (2007) 730–738.

[32] S.E. Lamhamedi-Cherradi, B.A. Menegaz, V. Ramamoorthy, D. Vishwamitra, Y. Wang, R.L. Maywald, et al., IGF-1R and mTOR blockade: novel resistance mechanisms and synergistic drug combinations for ewing sarcoma, Jnci-J. Natl. Cancer I. 108 (2016).

[33] Y.H. Yu, S.O. Yoon, G. Poulogiannis, Q. Yang, X.J.M. Ma, J. Villen, et al., Phosphoproteomic Analysis Identifies Grb10 as an mTORC1 Substrate That Negatively Regulates Insulin Signaling, Science 332 (2011) 1322–1326.

[34] P.D. Liu W.J. Gan H. Inuzuka A.S. Lazorchak D.M. Gao O. Arojo et al. Sinl phosphorylation impairs mTORC2 complex integrity and inhibits downstream Akt signalling to suppress tumorigenesis Nat Cell Biol. 15 2013 1340 U182.

[35] G. Yang, D.S. Murashige, S.J. Humphrey, D.E. James, A Positive feedback loop between Akt and mTORC2 via SIN1 phosphorylation, Cell Rep. 12 (2015) 937–943.

[36] M. Ladanyi, W. Pao, Lung adenocarcinoma: guiding EGFR-targeted therapy and beyond, Modern Pathol. 21 (2008) S16–S22.

[37] G.D. Guetz, B. Uzzan, K. Chouahnia, P. Nicolas, L. Zelek, M. Pailler, et al., Is there a benefit on survival of tyrosine-kinase inhibitors versus chemotherapy in first line in mutated Egfr patients with advanced non-small cell cancer (Nsclc)? A Meta-Analysis. Ann Oncol. 23 (2012) 414–425.

[38] S.M. Chen, C.L. Guo, J.J. Shi, Y.C. Xu, Y. Chen, Y.Y. Shen, et al., HSP90 inhibitor AUY922 abrogates up-regulation of RTKs by mTOR inhibitor AZD8055 and potentiates its antiproliferative activity in human breast cancer, Int J Cancer. 135 (2014) 2462–2474.

[39] N.E. Bhola, V.M. Jansen, J.P. Koch, H. Li, L. Formisano, J.A. Williams, et al., Treatment of triple-negative breast cancer with TORC1/2 inhibitors sustains a drug-resistant and notch-dependent cancer stem cell population, Cancer Res. 76 (2016) 440–452.

[40] J.O. Osanyingbemi-Obidi, C.M. Rudin, The roles of Notch signaling in the development of non-small cell lung cancer, Cancer Res. 71 (2011).

[41] B.J. Collins, W. Kleeberger, D.W. Ball, Notch in lung development and lung cancer, Semin Cancer Biol. 14 (2004) 357–364.

[42] J.S. Lim, A. Ibaseta, M.M. Fischer, B. Cancilla, G. O'Young, S. Cristea, et al., Intratumoural heterogeneity generated by Notch signalling promotes small-cell lung cancer, Nature 545 (2017) 360–364.

[43] A. Efstratiadis, M. Szabolcs, A. Klinakis, Notch, Myc and breast cancer, Cell Cycle 6 (2007) 418–429.

[44] R.E. Moellering, M. Cornejo, T.N. Davis, C. Del Bianco, J.C. Aster, S.C. Blacklow, et al., Direct inhibition of the NOTCH transcription factor complex, Nature 462 (2009) 182–188.

[45] B. D'Souza, L. Meloty-Kapella, G. Weinmaster, Canonical and non-canonical Notch ligands, Curr Top Dev Biol. 92 (2010) 73–129.

[46] C.F. Albright, R.C. Dockens, J.E. Meredith, R.E. Olson, R. Slemmon, K.A. Lentz, et al., Pharmacodynamics of Selective Inhibition of gamma-Secretase by Avagacestat, J Pharmacol Exp Ther. 344 (2013) 686–695.

[47] A.P. Weng, J.M. Millholland, Y. Yashiro-Ohtani, M.L. Arcangeli, A. Lau, C. Wai, et al., c-Myc is an important direct target of Notch1 in T-cell acute lymphoblastic leukemia/lymphoma, Gene Dev. 20 (2006) 2096–2109.

[48] B. Hoffman, D.A. Liebermann, Apoptotic signaling by c-MYC, Oncogene 27 (2008) 6462–6472.

[49] A. Wilson, F. Radtke, Multiple functions of Notch signaling in self-renewing organs and cancer, Febs. Lett. 580 (2006) 2860–2868.

[50] F. Radtke, K. Raj, The role of Notch in tumorigenesis: Oncogene or tumour suppressor? Nat. Rev. Cancer. 3 (2003) 756–767.

[51] Y. Ishikawa, I. Onoyama, K.I. Nakayama, K. Nakayama, Notch-dependent cell cycle arrest and apoptosis in mouse embryonic fibroblasts lacking Fbxw7, Oncogene 27 (2008) 6164–6174.

[52] X.D. Yang, R. Klein, X.L. Tian, H.T. Cheng, R. Kopan, J. Shen, Notch activation induces apoptosis in neural progenitor cells through a p53-dependent pathway, Dev. Biol. 269 (2004) 81–94.

[53] S. Romer, U. Saunders, H.M. Jack, B.M. Jehn, Notch1 enhances B-cell receptor-induced apoptosis in mature activated B cells without affecting cell cycle progression and surface IgM expression, Cell Death Differ. 10 (2003) 833–844.

[54] T. Morimura, R. Goitsuka, Y. Zhang, I. Saito, M. Reth, D. Kitamura, Cell cycle arrest and apoptosis induced by Notch1 in B cells, J. Biol. Chem. 275 (2000) 36523–36531.

[55] J. Konishi, K.S. Kawaguchi, H. Vo, N. Haruki, A. Gonzalez, D.P. Carbone, et al., Gamma-secretase inhibitor prevents Notch3 activation and reduces proliferation in human lung cancers, Cancer Res. 67 (2007) 8051–8057.

[56] N. Haruki, K.S. Kawaguchi, S. Eichenberger, P.P. Massion, S. Olson, A. Gonzalez, et al., Dominant-negative Notch3 receptor inhibits mitogen-activated protein kinase pathway and the growth of human lung cancers, Cancer Res. 65 (2005) 3555–3561.

[57] X. Yuan, H. Wu, H. Xu, N. Han, Q. Chu, S. Yu, et al., Meta-analysis reveals the correlation of Notch signaling with non-small cell lung cancer progression and prognosis, Sci. Rep. 5 (2015) 10338.

[58] Y. Zheng, C.C. de la Cruz, L.C. Sayles, C. Alleyne-Chin, D. Vaka, T.D. Knaak, et al., A rare population of CD24(+)ITGB4(+)Notch(hi) cells drives tumor propagation in NSCLC and requires Notch3 for self-renewal, Cancer Cell 24 (2013) 59–74.

[59] S. Adachi, A.J. Obaya, Z. Han, N. Ramos-Desimone, J.H. Wyche, J.M. Sedivy, c-Myc is necessary for DNA damage-induced apoptosis in the G(2) phase of the cell cycle, Mol. Cell Biol. 21 (2001) 4929–4937.

[60] Klefstrom J, Verschuren EW, Evan G. c-Myc augments the apoptotic activity of cytosolic death receptor signaling proteins by engaging the mitochondrial apoptotic pathway. J Biol Chem. 2002;277:43224-32.

[61] C.Y. Lin, J. Loven, P.B. Rahl, R.M. Paranal, C.B. Burge, J.E. Bradner, et al., Transcriptional amplification in tumor cells with elevated c-Myc, Cell 151 (2012) 56–67.

[62] Z.Q. Nie, G.Q. Hu, G. Wei, K.R. Cui, A. Yamane, W. Resch, et al., c-Myc is a universal amplifier of expressed genes in lymphocytes and embryonic stem cells, Cell 151 (2012) 68–79.

[63] D. Barsyte-Lovejoy, D.Y. Mao, L.Z. Penn, c-Myc represses the proximal promoters of GADD45a and GADD153 by a post-RNA polymerase II recruitment mechanism, Oncogene 23 (2004) 3481–3486.

[64] J. Si, X. Yu, Y. Zhang, J.W. DeWille, Myc interacts with Max and Miz1 to repress C/EBPdelta promoter activity and gene expression, Mol. Cancer. 9 (2010) 92.